

Analysis and simulation of the *in-situ* time-resolved reflectivity recorded during the growth of GaN on GaAs (110) substrate

Safa Othmani^a,^{ORCID} Imen Daldoul,^a Nouredine Chaaben,^{a,*} and Jean Paul Salvestrini^{b,c}^{ORCID}

^aMonastir University, Research Laboratory on Hetero-Epitaxies and Applications, Faculty of Sciences, Monastir, Tunisia

^bGeorgia Tech Lorraine, International Research Lab Georgia Tech – CNRS (IRL 2958), Metz, France

^cGeorgia Institute of Technology, School of Electrical and Computer Engineering, Atlanta, Georgia, United States

ABSTRACT. The growth rate of GaN on the GaAs (110) substrate as deduced from reflectivity measurements exhibits a peculiar behavior. A transient regime with a relatively high initial growth rate progressively decreases to a limit value during the early stage of high temperature GaN growth. An optical model, incorporating time-dependent profiles of the growth rate and surface roughness, was used to simulate the corresponding *in situ* reflectivity recorded during the growth of GaN layers on the GaAs (110) substrate. The growth rate transient, characterized by a time constant (τ) and a diffusion length (L), is proposed to originate from Ga self-diffusion in the GaN layer. Both the time constant (τ) and the diffusion length (L) increase with the rising growth temperature. This allows for the estimation of the Ga self-diffusion coefficient in GaN, which, in the growth temperature range of 750°C to 900°C, was found to be equal to $D = 1.35 \cdot 10^{-11} \exp(-(0.28 \pm 0.04)/k_B T) \text{ cm}^2 \text{ s}^{-1}$.

© The Authors. Published by SPIE under a Creative Commons Attribution 4.0 International License. Distribution or reproduction of this work in whole or in part requires full attribution of the original publication, including its DOI. [DOI: [10.1117/1.OE.63.1.014104](https://doi.org/10.1117/1.OE.63.1.014104)]

Keywords: optical recording; *in situ* reflectance; optical modeling; simulation; epitaxy; Ga self-diffusion

Paper 20230772G received Aug. 26, 2023; accepted Dec. 21, 2023; published Jan. 11, 2024.

1 Introduction

The metal organic vapor phase epitaxy (MOVPE) of GaN has been intensively studied on the GaAs substrate. GaN growth on GaAs is a typical example of high lattice-mismatched substrates. Despite the progress made on the optimization of cubic GaN growth on a GaAs substrate, the GaN material often coexists in both the cubic and hexagonal phases. The origin of the hexagonal phase is related to the structural defects emerging during the GaN growth, such as the interfacial roughness, dislocations, and amorphous phase inclusions. Many studies on the subject are focused on the growth process of high quality cubic GaN, which is interesting for research purpose as it presents a direct band gap of 3.23 eV at room temperature and a centrosymmetric lattice.^{1,2} Although the properties such as small effective masses, high doping efficiency, and high carrier mobility are attractive, the interest in the cubic GaN is limited because of the difficulties involved in its growth. For example, it is possible to grow cubic GaN epilayers on the GaAs (001) substrate, but the nitridation condition of the surface strongly impacts the quality of the GaN layer, leading to the presence of wurtzite phase inclusions when there is excessive or insufficient nitridation.³ The used parameters to grow cubic GaN are very

*Address all correspondence to N. Chaaben, nouredine.chaaben@fsm.rnu.tn

critical, so the growth process plays a fundamental role in investigating the epitaxial mechanisms that govern the phase purity of cubic GaN. The growth of GaN by MOVPE takes place in four stages: adsorption, diffusion, desorption, and incorporation of gallium (Ga) and nitrogen (N) active species. The diffusion of active species is the most important phenomena for determining the growth kinetic and mode. In particular, the surface diffusion of the Ga and N species may significantly influence the growth rate. The diffusion of Ga and N over the GaAs surface is related to the growth temperature and initial nitridation process. The presence of defects at the GaN/GaAs interface in the GaN nucleation layer on the GaAs substrate strongly depends on the two parameters.⁴ Previously, we studied the growth temperature (750°C to 900°C) effect on the structural and optical properties of GaN on a GaAs (110) substrate.⁵ The results proved that GaN properties are very different in this growth temperature range. We found that GaN has a polycrystalline structure with a preferential alignment of cubic GaN according to a (220) orientation at 850°C. The results also showed a cubic GaN emission at 3.23 eV for this growth temperature and a major hexagonal GaN emission for 900°C as the extreme growth temperature.

The *in situ* real time monitoring by laser reflectometry of epitaxial growth gives potential information on the kinetic growth of film, such as the growth rate, thickness, and surface roughness. In particular, using a wave length $\lambda = 632.8$ nm of the laser source, the *in situ* time reflectivity of the GaN epilayer on the GaAs substrate shows good contrast due to the large difference between their refractive index ($n_{\text{GaN}} = 2.39^6$ and $n_{\text{GaAs}} = 3.86^7$) and the very low extinction coefficient of GaN ($k_{\text{GaN}} = 0.008$).⁶ The relatively high extinction coefficient of the GaAs substrate ($k_{\text{GaAs}} = 0.2$ ⁷) does not affect the contrast of reflectivity. So far, we have developed and used several optical models of the reflectivity for different purpose.⁸⁻¹³ In a recent attempt to simulate the reflectivity of GaN layers grown on a GaAs (110) substrate, singular reflectivity signals were observed. Indeed, the reflectivity revealed the presence of a transient regime during the early stages of high temperature GaN growth followed by a steady-state regime. The transient regime was marked by a relatively high initial growth rate that progressively decreases down to a limit value.

Previously, we used the optical model, as described above, to simulate the *in-situ* reflectivity signals recorded during the MOVPE of GaN on SiN treated sapphire¹¹ and GaAs^{12,13} substrates. In these references, based on morphological observations of growth mode transitions, we suggested different profiles of the growth rate $v(t)$ and surface roughness $\sigma(t)$: 3D-2D in the case of GaN growth on the SiN treated sapphire substrate and 2D-3D in the case of GaN nucleation layers grown on (100), (113), (112), and (111) oriented GaAs substrates. The growth of GaN on GaAs (110) was performed under H₂ carrier gas with a 50 nm thick GaN buffer layer and without nitridation of GaAs (110).⁵ These growth conditions are different from those used on (100), (113), (112) and (111) oriented GaAs substrates,^{12,13} where N₂ was used as the carrier gas and the GaAs substrate underwent a nitridation step before the growth of the GaN nucleation layer. Unlike the case in Refs. 12 and 13, which show time-dependent profiles of increasing growth rate and increasing surface roughness, the early stages of GaN grown on GaAs (110) also showed a 2D-3D transition mode, but with time-dependent profiles of a decreasing growth rate and increasing surface roughness.

The origin of the high initial growth rate in the case of GaN growth on a GaAs (110) substrate could be attributed to the Ga diffusion from the GaAs substrate, which starts to decompose at high temperatures. This could give rise to an excess of Ga, which could contribute to the GaN growth in the early stages.

In this paper, the important finding is the determination of the Ga self-diffusion coefficient in GaN in the temperature range of (750°C to 900°C) from the simulation of the *in situ* reflectance-time signals recorded during the growth of GaN layers on the GaAs (110) substrate. We show that the analysis of the different growth rate profiles with an appropriate choice of interdependent growth rate and surface roughness profiles could lead to the determination of the Ga self-diffusion in GaN. The proposed indirect approach is simple and allows for overcoming the issues faced in the more direct measurement of the self-diffusion coefficient based on the diffused radioactivity in isotope heterostructures such as in the case of Ga self-diffusion in GaAs¹⁴ or nitrogen self-diffusion in GaN.¹⁵ Furthermore, the Ga self-diffusion in GaN is rarely studied experimentally.

2 Experimental Details

GaN layers were grown on the GaAs (110) substrate by MOVPE. The growth temperature was measured with an S-type thermocouple inserted into a fixed graphite susceptor. The reactor was a quartz cylinder that was 45 cm long and 5.5 cm in diameter. The used GaAs (110) substrates were cut from the same wafer and had a surface ranging from 1 to 2 cm². The substrates have square, triangular, or trapezoidal shapes. Trimethylgallium (TMG) and ammoniac (NH₃) were used as gallium (Ga) and nitrogen (N) sources, respectively. GaN growth was carried out in atmospheric pressure using H₂ as the carrier gas for the growth of GaN layers. A series of 1 μm thick-GaN layers was grown at different growth temperature in the range of 750°C to 900°C on a GaAs (110) substrate using a 50 nm thick-GaN buffer layer grown at 550°C. The GaAs substrate does not undergo any nitridation step. In addition, to avoid decomposition of the GaAs surface, we used a relatively high growth rate close to 2 μm/h (33 nm/min). The thickness of the GaN buffer layer (50 nm) is sufficient for completely covering the GaAs surface.

More details about the growth process and properties of GaN layers grown on GaAs (110) substrates have been reported elsewhere.⁵ The GaN layers grown at temperatures of 750°C, 800°C, 850°C, and 900°C are noted A, B, C, and D, respectively. The growth process was *in-situ* monitored by He-Ne laser reflectometry under normal incidence light ($\lambda = 632.8$ nm). The size of the laser beam on the surface of the GaN layer being deposited is around 3 mm². The reflectivity signal was recorded by a silicon detector with a 5 mm radius of the sensitive surface. The surface morphology of GaN layers was analyzed by an atomic force microscope (AFM). We used spectral reflectance in UV-visible range for thickness measurements. The optical properties of GaN layers were investigated using room temperature cathodoluminescence (CL).

3 Optical Models

First, we must point out that, in the case of normal incidence and a smooth surface film growing on the substrate, the complex reflectance amplitude is given as^{6,8-13}

$$r(t) = \frac{r_{1f} + r_{fs} \exp\left(-\frac{i4\pi N_f d(t)}{\lambda_0}\right)}{1 + r_{1f} r_{fs} \exp\left(-\frac{i4\pi N_f d(t)}{\lambda_0}\right)}, \quad (1)$$

and the reflectance signal versus growth time is given as

$$R(t) = |r(t)|^2, \quad (2)$$

where r_{1f} and r_{fs} are the Fresnel reflection coefficients at smooth air/film and film/substrate interfaces, respectively, and are defined as

$$r_{1f} = \frac{1 - N_f}{1 + N_f}, \quad (3)$$

and

$$r_{fs} = \frac{N_f - N_s}{N_f + N_s}, \quad (4)$$

where $N = n - ik$ is the complex refractive index of the film (N_f) and substrate (N_s). n is the real part of the refractive index, and k is the extinction coefficient of materials. The refractive index of the ambient gas was assumed to be equal to 1. We consider, at the used wavelength, $n_s = 3.86$ and $k_s = 0.20$ as refractive index and extinction coefficient values of the GaAs substrate, respectively.⁷ The optical constants (n, k) of the GaN layer were used as simulation parameters.

A virtual interface model developed by Breiland et al.⁸ has been applied to multilayer structures with optically smooth surfaces and interfaces. Then, Chaowang et al.⁶ developed a quantitative analysis model to incorporate time-dependent light scattering by a rough surface and a time-dependent vertical growth rate during growth on a rough surface into the virtual interface model.

In the case of a rough surface film growing on the substrate, effective Fresnel coefficients were adopted for a rough GaN surface, as proposed by Szczyrbowski et al.¹⁰ These are given by

Eqs. (5)–(10), in which the modifications factors $\alpha(t)$, $\beta(t)$, and $\gamma(t)$ are functions of the surface roughness $\sigma(t)$ of film, the refractive index of film, and the wavelength used for monitoring, given as

$$r'_{1f} = r_{1f}\alpha(t), \quad (5)$$

$$\alpha(t) = \exp\left\{-2\left[\frac{2\pi\sigma(t)}{\lambda_0}\right]^2\right\}, \quad (6)$$

$$r'_{f1} = r_{f1}\beta(t), \quad (7)$$

$$\beta(t) = \exp\left\{-2\left[\frac{2\pi\sigma(t)}{\lambda_0}\right]^2 n_f^2\right\}, \quad (8)$$

$$t'_{1f} = t_{1f}\gamma(t), \quad (9)$$

$$\gamma(t) = \exp\left\{-\left(\frac{1}{2}\right)\left[\frac{2\pi\sigma(t)}{\lambda_0}\right]^2 (n_f^2 - 1)\right\}. \quad (10)$$

The modification factors become time dependent through the time dependence of the surface roughness $\sigma(t)$.

The complex reflectance amplitude is given as^{6,10–13}

$$r'(t) = \frac{r_{1f}\alpha(t) + r_{fs}[\gamma^2(t) + r_{f1}^2(\alpha(t)\beta(t) - \gamma^2(t))]\exp\left(-\frac{i4\pi N_f d(t)}{\lambda_0}\right)}{1 + r_{1f}r_{fs}\beta(t)\exp\left(-\frac{i4\pi N_f d(t)}{\lambda_0}\right)}, \quad (11)$$

and the reflectivity signal versus growth time is given as

$$R'(t) = |r'(t)|^2. \quad (12)$$

To give good simulations of reflectivity recorded during the growth of GaN on GaAs (110), we suggest the following growth rate $v(t)$ and surface roughness $\sigma(t)$ profiles, as expressed in Eqs. (13)–(15). The suggested profile of surface roughness was supported by the AFM analyses.

$$v(t) = v_s + v_d e^{-\left(\frac{t-t_0}{\tau}\right)}, \quad (13)$$

$$\sigma_0(t) = \sigma_1 - (\sigma_1 - \sigma_i) e^{-\left(\frac{t-t_0}{\tau}\right)}, \quad (14)$$

$$\sigma(t) = \sigma_0(t) e^{-\left(\frac{t-t_0}{\tau_d}\right)}, \quad (15)$$

where τ and τ_d are the time constants of the transient regime and damping, respectively. The surface roughness profile $\sigma_0(t)$ describes the transient regime for the GaN growth. v_d and v_s are the dynamic growth rate and the static growth rate, respectively. At the start time t_0 , the initial growth rate is given by $v_i = v_s + v_d$. The thickness of the GaN layer is given by Eq. (16), where d_{c0} is the initial thickness at the start time of simulation (t_0):

$$d(t) = d_{c0} + \int_{t_0}^t v(t) dt. \quad (16)$$

4 Results and Discussion

Figure 1 shows the AFM ($5 \times 5 \mu\text{m}^2$) images of both the GaN buffer layer [Fig. 1(a)] and GaN sublayers grown at 850°C on top of the buffer layer [Figs. 3(b) and 3(c)].

The root mean square (RMS) roughness and the island size distribution were extracted from these AFM images. By comparing the roughness profiles of layers C_1 and C , we observed that the high density and small lateral size islands in the GaN buffer layer turn into lower density and larger lateral size of islands in the thick GaN layer. The larger RMS of the thick GaN layer could be associated with a partial coalescence of the GaN islands in the last growth stages. However, we can see a slight difference between the profiles of buffer layer C_0 and layer C_1 in terms of the

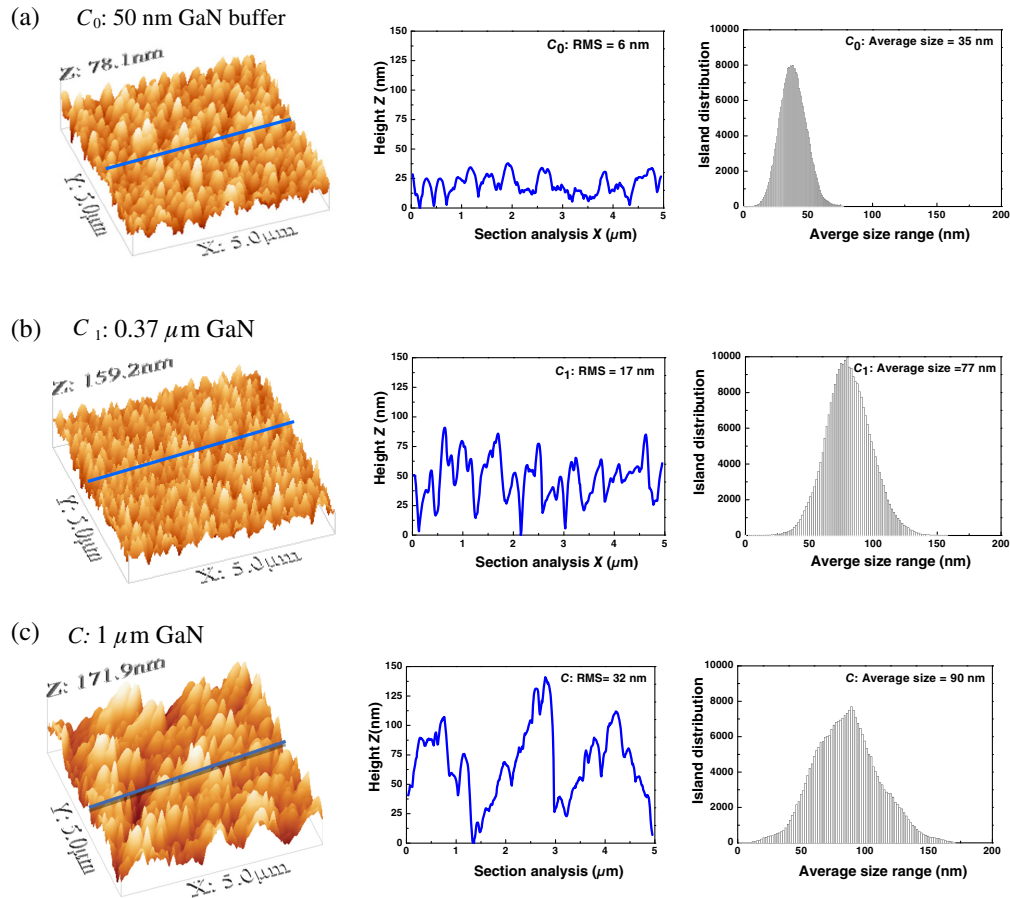


Fig. 1 $5 \times 5 \mu\text{m}^2$ AFM surface images and corresponding profiles and height distributions of GaN islands of (a) C_0 (50 nm thick GaN buffer layer grown at 550°C on GaAs (110) substrate), (b) C_1 (0.37 thick GaN sublayer), and (c) C (1 μm thick GaN sublayer). The sublayers C_1 and C were grown at 850°C using a 50 nm thick GaN buffer layer grown under the growth conditions of C_0 .

density and lateral size of the islands. The RMS roughness for the layers C_0 , C_1 , and C were 6, 17, and 32 nm, respectively. The RMS roughness is increased by a factor of 2.8 and 1.9 for a thickness of 0.37 and 1 μm , respectively. These values indicate a rapid increase in the surface roughness in the early growth stages compared with the last growth stages. The figures on the right of Fig. 1 show the height distributions of islands as extracted from the AFM data. The average vertical sizes for layers C_0 , C_1 , and C were 35, 77, and 90 nm, respectively. The average vertical size is increased by a factor of 2.2 and 1.2 for a thickness of 0.37 and 1 μm , respectively. These values also indicate a rapid increase of the average vertical size of islands in the early growth stages. By correlating between the evolutions versus the thickness of the surface roughness and average vertical size, the rapid increase of the surface roughness could be associated with a rapid increase in the vertical size of islands in the early growth stages. The increase of the vertical size can be limited by the coalescence of islands. However, the size dispersion also contributes to the roughness increase. The full width at half maximum (FWHM) of the island distribution was 25, 38, and 56 nm for layers C_0 , C_1 , and C , respectively. The FWHM varies by a factor close to 1.5 in the early and last growth stages. Layer C shows the coexistence of two island size distributions, which can be associated with the presence of hexagonal inclusions in the thick cubic GaN layer.⁵

Figure 2 shows the *in-situ* reflectivity signals recorded for the series of samples A-D as well as their corresponding fits using the above model.

Experimental reflectivity data were collected with a typical data interval of ~ 2 s. All reflectivity signals were normalized with respect to one of the substrates (R_s). The start time ($t_0 = 0$) of simulations was taken at the first minimum reached by the reflectance signal after the run of

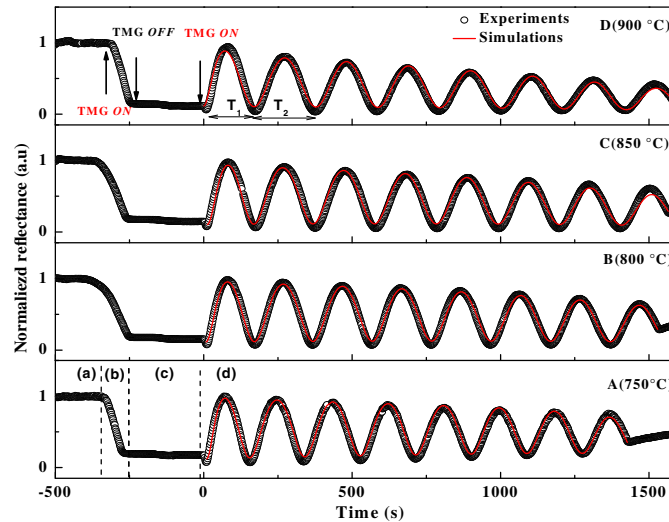


Fig. 2 Plots of experimental data (open circles) and simulation (solid lines) reflectance corresponding to layers A, B, C, and D grown at growth temperatures 750°C, 800°C, 850°C, and 900°C, respectively. The growth steps are as follows: (a) the temperature ramping from ambient to 550°C; (b) the growth of GaN buffer layer, which starts by the first TMG ON and ends by the first TMG OFF, with in this step the decrease of reflectivity being due to the thickness increase; (c) the interruption of growth and temperature ramping from 550°C to 850°C (short annealing of the buffer layer), with in this step the reflectivity remaining almost constant; and (d) the growth of 1 μm thick GaN sublayer, which starts by the second TMG ON when the temperature is established. After the second set of TMG flux, the reflectivity of the GaN sublayer shows a rapid oscillation (a decrease in a narrow domain of thickness (50 to 65 nm) to reach the first minimum, followed by an increase and oscillations, etc.), indicating a progressive increase of thickness. The oscillation period measurements from the minima given $T_1 < T_2$.

TMGa flux. This time corresponds to a thickness of both the buffer layer and sublayer equal to 65 nm, which is equivalent to a half-period of time. All of the reflectivity signals exhibit oscillations, and their amplitudes decrease with the growth time. This damping is synonymous with the progressive increase of the surface roughness, which causes the scattering of the laser beam. The damping degree increases with the increasing growth temperature. For the highest temperature 900°C, the oscillations remain pronounced until the growth of a thickness close to 1 μm . This indicates that the surface degradation is not significant compared with GaN layers with a surface roughness close to 90 nm for which the reflectivity is close to zero.¹¹

To study the damping of reflectivity and highlight the difference between the two effects of surface roughness and absorbance, we conducted a quantitative study on the experimental reflectivity curves of layers A–D. This study is based on the measurements of extrema (max and min) as well as the average (*av*) of reflectivity. These measurements were compared with those of the theoretical reflectivity of the smooth GaN layer, which is calculated using Eq. (1)–(2) and the realistic values of optical constants ($n = 2.39$, $k = 0.008$) and growth rate ($v = 2.55 \mu\text{m}/\text{h}$). Figure 3 shows the evolutions versus thickness of the minimum, maximum, and average of the experimental reflectivity (R_{exp}) of layers A–D and those of the theoretical reflectivity (R_{theo}).

At the early growth stages of the GaN sublayer, the differences between the average reflectivity values are associated with the differences between the values of the initial surface roughness. When the thickness of the GaN layer increases, the decrease of the average reflectivity as well as the maximum is associated with the surface roughness increase. These decreases become more pronounced when the growth temperature is increased. For the low temperature of 750°C (layer A), we observed that the minimum increases from 0.04 to 0.15 when the thickness is increased from 0.065 to 1 μm . For layer A, the minimum value is close to that of the theoretical reflectivity at a thickness of 1 μm . The minimum increase is associated with the absorbance increase of the GaN layer, which is related to the extinction coefficient (k) and thickness (d) (increase of $k \cdot d$). Layers B, C, and D showed almost the same constant value of the minimum with the thickness increase. The minimum values are comparable and vary from 0.02 to 0.04. The

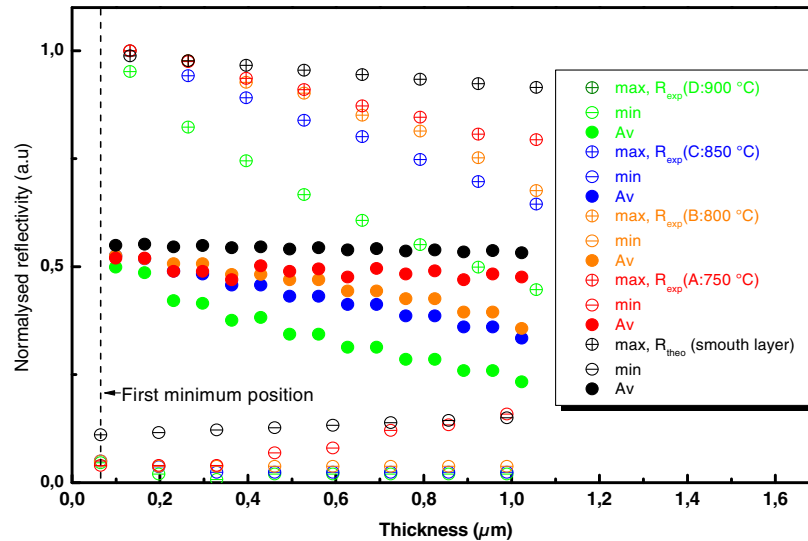


Fig. 3 Plots of extrema (max and min) and average of experimental reflectivity (R_{exp}) of layers (A), (B), (C), and (D) compared with those of theoretical reflectivity (R_{theo}) calculated for the smooth GaN layer using Eqs. (1) and (2) and realistic values of optical constants ($n = 2.39$, $k = 0.008$).

constant value of the minimum is due to the compensation of the absorbance by the surface roughness increase. The minimum decrease should be observed for a higher surface roughness.

By comparing periods T_1 and T_2 ($T_1 < T_2$) for all experimental reflectivity curves (see Fig. 2), we clearly observe the presence of the relatively high initial growth rate. This high value of the initial growth rate at the early growth stages is essentially due to the excess of gallium coming from the decomposition of GaAs substrate. The amount of excess gallium diffuses through the buffer layer and the sublayer being deposited. The GaAs (110) decomposition was enhanced using H_2 carrier gas and the absence of nitridation of the substrate compared with the results reported in previous works.¹²⁻¹³ The growth temperature range below 900°C ensures the GaN thermal stability on GaAs but does not prevent the GaAs decomposition below the GaN layer being deposited. Regarding the presence at the early growth stages of a high initial growth rate followed by the damping of the reflectivity with constant growth rate, we assume the existence of two regimes. The first regime (transient regime: I) was characterized by a first-time constant (τ) indicating an interdependence between the growth rate and surface roughness profiles. In this regime, the growth rate shows an exponential decay, and the surface roughness changes to reach a limit value (σ_1). The second regime (steady regime: II) was characterized by a second time constant (τ_d) indicating a damping of the reflectance time due to the surface roughness increase versus thickness. In this regime, due to the increase of the vertical size of the GaN islands, the growth mode gradually undergoes 2D-3D transition with a constant growth rate (static growth rate: v_s). Because of the presence of growth rate profile, the progressive thickness $d(t)$ of the GaN layer shows a nonlinear increase versus growth time for the first regime, whereas it follows a linear law with a slope that gives the static growth rate (v_s) for the second regime. Xu et al.¹⁶ also showed a growth rate decrease with growth time during MOVPE of GaN on the GaAs (100) substrate. They used triethylgallium (TEGa) as the Ga source, and they associated the high initial growth rate with Ga diffusion through the GaN film. The authors reported that the diffusion length of Ga in GaN was close to $L = 0.26 \mu\text{m}$ at growth temperature $T_g = 800^\circ\text{C}$. By comparison, for the same growth temperature, we found a diffusion length of Ga close to $L = 0.062 \mu\text{m}$, which is four times lower than the value reported by Xu et al.¹⁶ This difference could be explained by the difference between the growth rate value, which is lower in the case of using TEGa as the Ga source.¹⁷ The growth rate profile becomes more obvious for lower growth rates. As mentioned in the experiments, the initial high growth rate is useful in buffering the lower growth step to avoid decomposition of the GaAs surface. The GaN buffer layer thickness close to 50 nm completely covers the GaAs surface, but As and Ga still diffuse during two growth steps of the GaN buffer layer and high temperature GaN sublayer.

To give best simulations of the reflectance-time curves of the GaN/GaAs (110) layers, based on the presence of the two regimes described above, we suggest the growth rate and surface roughness profiles as given by Eqs. (13)–(15). The best fits of the reflectivity curves are also plotted in Fig. 2. The corresponding parameters are summarized in Table 1. For the thickness dependence of the growth rate, we used the following equation:

$$v(d) = v_s + v'_d e^{-\left(\frac{d-d_0}{L}\right)}, \quad (17)$$

where L is a diffusion length and v'_d is a dynamic growth rate.

As shown in Table 1, we notice a small reduction of the static growth rate (v_s) in the growth temperature range of 750°C to 900°C from 2.55 to 2.23 $\mu\text{m}/\text{h}$ (by order of 10%). This small reduction of static growth rate may be associated with the reducing effect of hydrogen used as the carrier gas.¹⁸ To have a better insight on the different growth rate evolution, we introduce the relative growth rate (RGR) as

$$R(\%) = 100 \cdot \frac{v(t, d) - v_s}{v_s}, \quad (18)$$

where $v(t, d)$ is the growth rate at time t or thickness d coming from the fits of the data of Fig. 2. Figures 4(a) and 4(b) show the dependences of RGR and their corresponding fits versus time and thickness, respectively.

In Fig. 4(b), the fit of the average growth rate data points was done using Eq. (17) and starts from the layer thickness of 0.099 μm . We clearly observe a relatively high initial growth rate, which then decreases and reaches a constant value.

The thicknesses of the GaN layers were also *ex-situ* determined from the oscillations of the reflectance spectra using several periods, given as⁶

$$d = \frac{\lambda_1 \lambda_2}{2(\lambda_1 n_2 - \lambda_2 n_1)}, \quad (19)$$

where λ_1 and λ_2 are the wavelengths for two adjacent extrema of the same type and n_1 and n_2 are the corresponding refractive index. The thickness values given from the reflectance spectra (see Table 1) are in good agreement with those found by simulations of the reflectivity.

Table 1 Parameters of output simulations related to layers A-D with thickness and surface roughness values given by UV-visible spectral reflectance (SR) and AFM analysis, respectively.

Output simulations	Layer			
	A (750°C)	B (800°C)	C (850°C)	D (900°C)
Refractive index n	2.40	2.39	2.38	2.38
Extinction coefficient k	0.012	0.008	0.008	0.008
Initial surface roughness σ_i (nm)	6	8	11	15
Initial growth rate $v_i = v_s + v_d$ ($\mu\text{m}/\text{h}$)	3.85	3.87	3.96	3.98
Final growth rate $v_f = v_s$ ($\mu\text{m}/\text{h}$)	2.55	2.37	2.30	2.23
Time constant τ (s)	54	64	85	88
Damping time τ_d (s)	2720	2190	1840	1550
Characteristic parameters				
Final surface roughness σ_f (nm)	27	33	40	54
AFM surface roughness (nm)	19	25	32	37
Final thickness d (μm) (simulation)	1.00	1.05	1.08	1.05
Measured thickness d (μm) (SR)	1.04	1.11	1.15	1.06

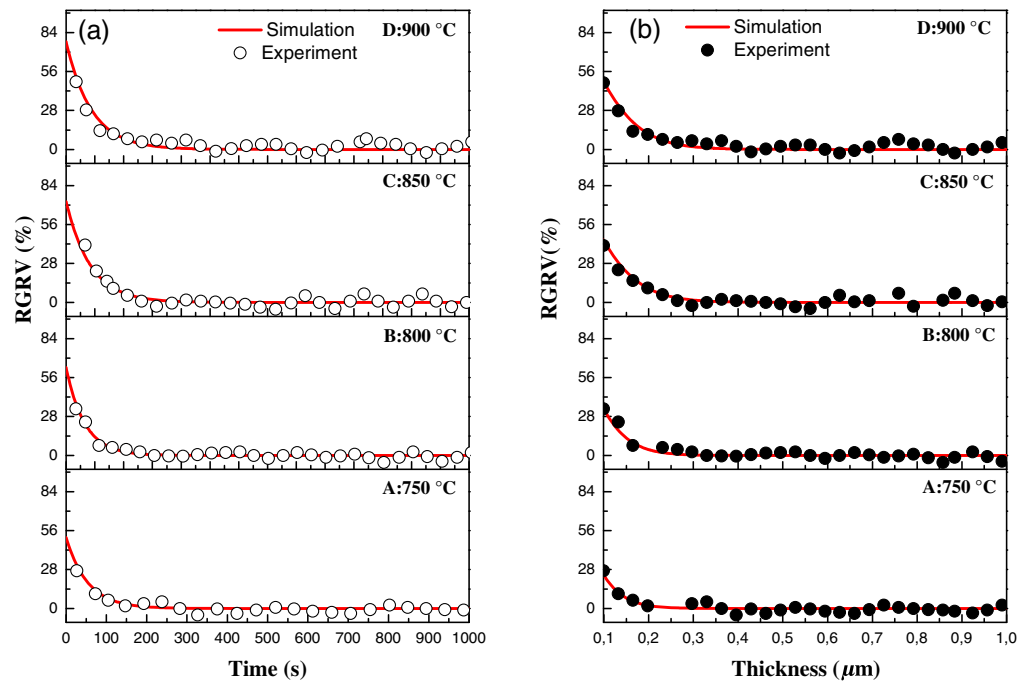


Fig. 4 (a) Plots of growth rate profiles versus growth time, from the start time ($t_i = 0$) giving the best simulation of reflectance-time curves of layers A, B, C, and D. (b) The corresponding growth rate profile versus the progressive thickness, given by fitting of experimental average growth rate data using Eq. (17). The open and full circles correspond to the average growth rates, calculated from the oscillations periods of reflectance-time curves, versus average extremum time $((T_i + T_{i+1})/2)$ and versus the corresponding thickness. The average growth rate calculus starts from the layer thickness $d_{e0} + 0.033 = 0.099 \mu\text{m}$ corresponding to the growth time close to $T_1/4$ from the start time simulation ($t_0 = 0$).

Figure 5 shows reflectance spectra performed in the UV-visible range (300 to 900 nm) at the left side (1), in the center (2), and at the right side (3) of layer C surface, as marked in the inset photo.

We clearly see that there are little differences between the three spectra, in terms of contrast and periods in the entire domain of wavelength (300 to 900 nm). The measurement of the average thickness showed a small difference ($d = 10 \text{ nm}$) between the values measured in the three

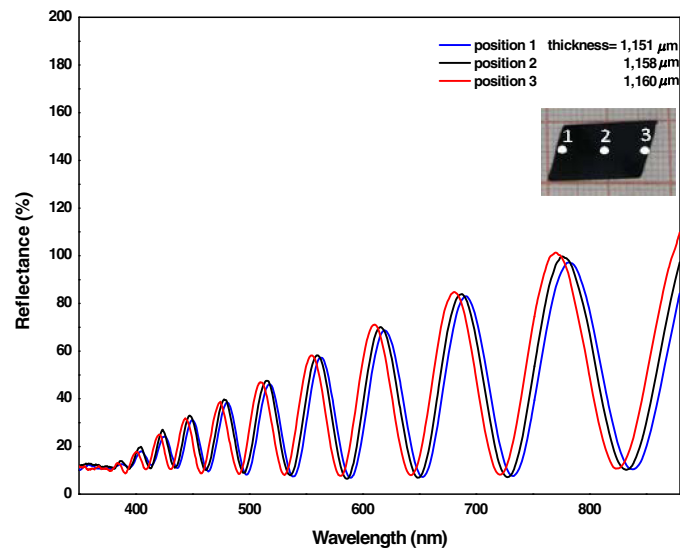


Fig. 5 Reflectance spectra in the UV-Visible range (300 to 900 nm) at the left side (1), in the center (2) and at the right side (3) on the layer C surface (photo inset of figure).

positions (1, 2, and 3). Figure 6 shows the surface and cross-section views of SEM images corresponding to a GaN layer grown at 850°C.

Figure 6(a) shows a three dimensional (3D) homogenous growth mode with a preferential orientation of cubic GaN islands. Figure 6(b) shows the cross-section view of an SEM image that also indicates a good interface between the GaN layer and GaAs substrate and a homogenous thickness of GaN. At a higher growth temperature of 900°C, the surface morphology showed a

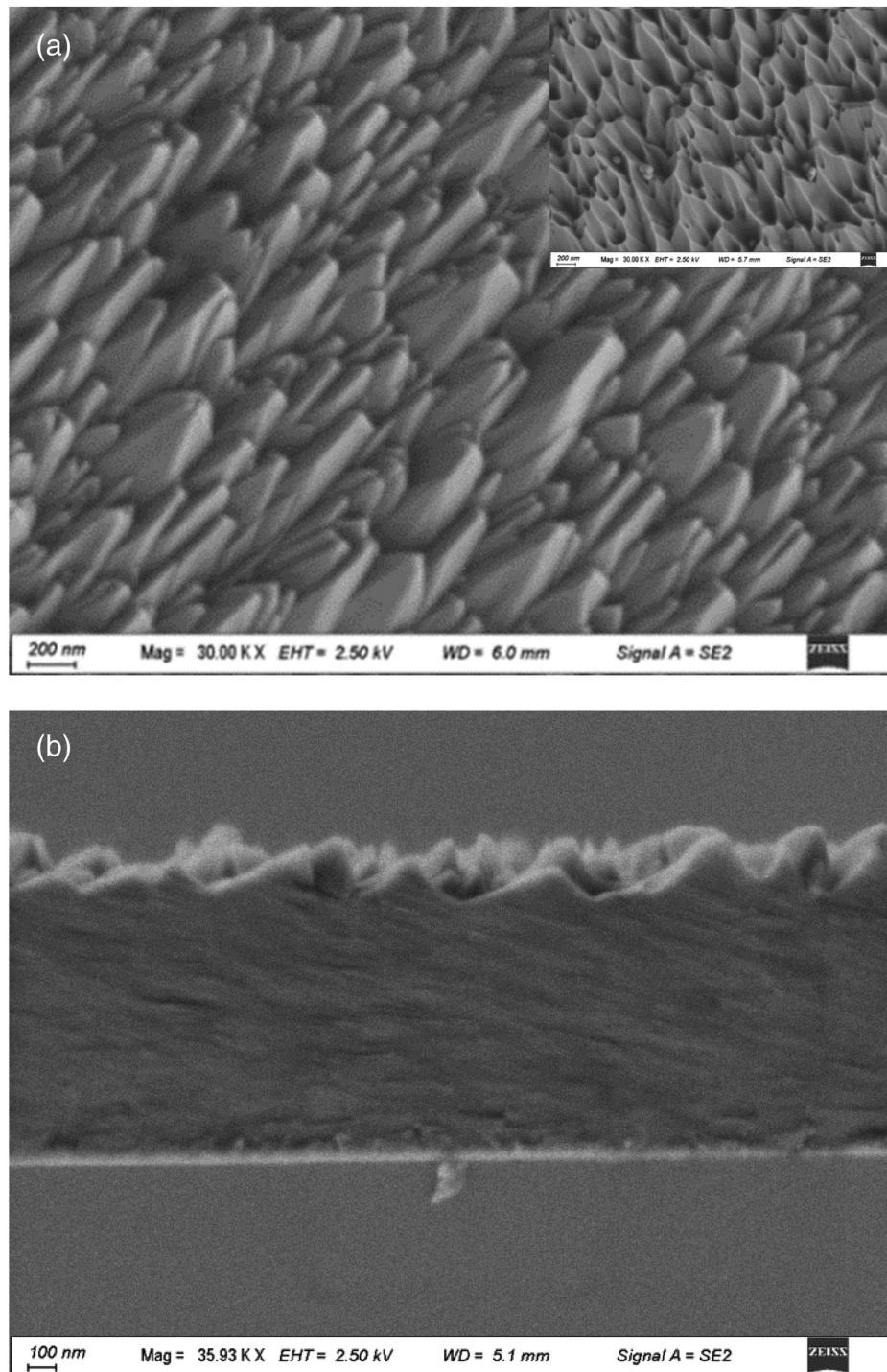


Fig. 6 Surface and cross-section view of SEM images corresponding to the GaN layer grown at 850°C (layer C). The inset of panel (a) shows the surface morphology of the GaN layer grown at 900°C (layer D).

similar porous structure, as seen in the inset of Fig. 6(a), which we associated with diffusion of the As element through the GaN layer.⁵

Figure 7 shows CL spectra recorded at room temperature and for a beam energy of 20 keV in the GaN layers grown at 850°C and having a thickness varying from 0.15 to 1 μm .

All spectra are normalized with respect to the magnitude of the GaN defect band (yellow band: YB) entered around 2.4 eV. All spectra exhibit a peak centered at around 3.23 eV corresponding to the cubic GaN. Table 2 gives the position, intensity, and FWHM for each peak of band edge emission. In the thickness range, the position and intensity values show slight

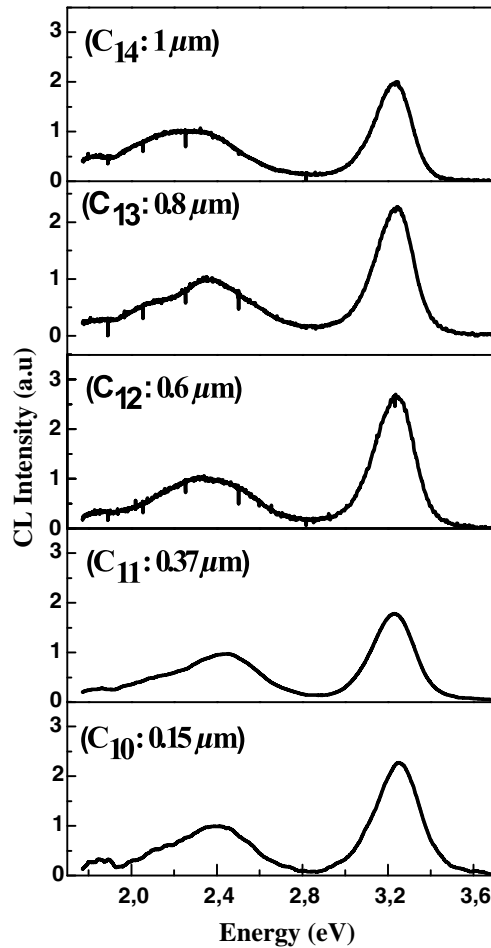


Fig. 7 CL spectra (normalized with respect to the yellow defect band intensity) of GaN epilayers grown at 850°C with the thickness varying from 0.15 to 1 μm . The CL spectra were recorded at room temperature with a beam energy of 20 keV.

Table 2 Peak position, intensity, and FWHM of cathodoluminescence evolutions versus thickness of the GaN epilayer grown at 850°C.

Layer	Thickness (μm)	Peak position (eV)	Intensity (a.u)	FWHM (meV)
C_{10}	0.15	3.25	2.2	234
C_{11}	0.37	3.23	1.8	233
C_{12}	0.60	3.23	2.6	208
C_{13}	0.80	3.24	2.3	204
C_{14}	1.00	3.23	2.1	200

fluctuations around 3.23 eV and 2, respectively. The FWHM values indicate a slight improvement of optical properties of the cubic GaN layer with the thickness increase. These results show that the optical properties of cubic GaN layers grown at 850°C with different thicknesses are very comparable.

Figure 8 shows the surface roughness profiles that led to the best simulations of experimental reflectivity of layers A–D.

During the transient regime, the surface roughness profile shows a rapid increase toward a limit value (σ_1) according to Eq. (14); then it shows an exponential increase, according to Eq. (15). The surface roughness profile was characterized by two constants of time. The first time constant (τ) corresponds to an interdependence between profiles of the growth rate and surface roughness in the transient regime. The second time constant (τ_d) corresponds to the damping regime of the reflectivity. These results are in good agreement with the AFM analyses. In the transient regime, the Ga diffusion coming from the TMGa precursor becomes less important than the excess Ga coming from the GaAs decomposition. This could favor high density of islands and consequently delay their coalescence. This induces a columnar structure with a rapid increase of surface roughness in the transient regime. We associate the rapid increase of roughness with the high initial growth rate. At the early growth stages, due to the vertical Ga diffusion

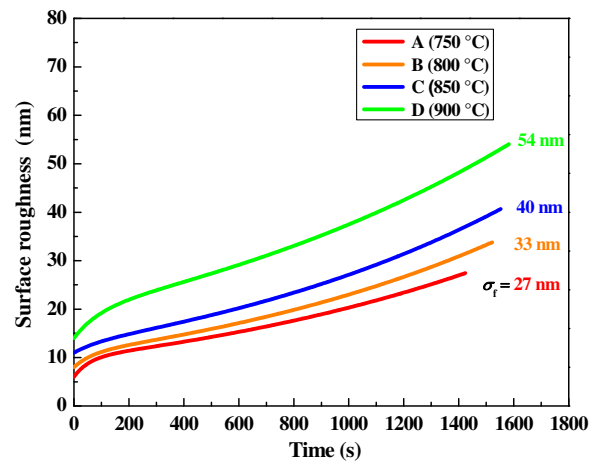


Fig. 8 Plots of surface roughness profiles giving the best simulations of the experimental reflectivity of layers A, B, C, and D grown at different temperatures. For each profile, we inserted the final surface roughness values reached at the growth end.

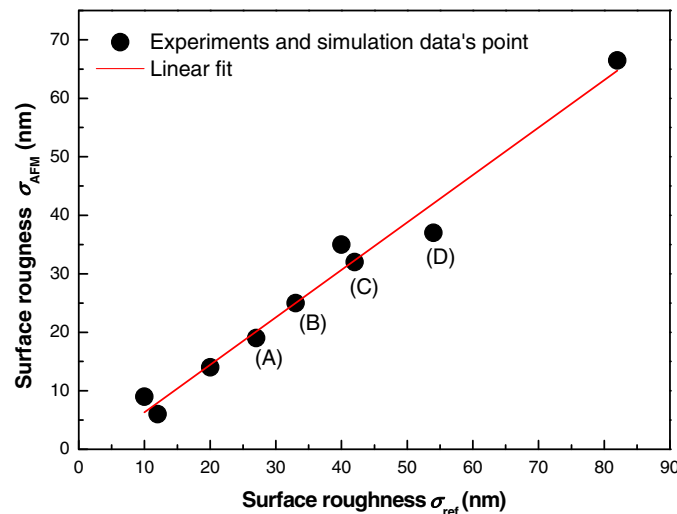


Fig. 9 Variation of the surface roughness given by AFM versus surface roughness given by the simulation of reflectance-time curves. The points A, B, C, and D correspond to layers A–D, respectively.

through the GaN layer, a local growth mode can take place, leading to the increase of vertical size islands. During the second regime, the progressive increase of the layer thickness was accompanied by an increase of the island size according to the Stranski-Krastanov (SK) growth mode.¹⁹ As shown in Fig. 7, the increase of final surface roughness with growth temperature is associated with the increase of island size and their dispersion.

Figure 9 shows the plot of surface roughness given by AFM (σ_{AFM}) versus surface roughness given by the fits of reflectivity curves [σ_{ref} : final surface roughness (σ_f) in Table 1].

The data points related to layers A–D are marked by the corresponding letters. We get a linear law between σ_{AFM} and σ_{ref} . Analogous observations have been reported in other studies.^{20,21}

5 Ga Self-Diffusion in GaN

From the simulation results as seen in Figs. 4(a) and 4(b), we determine the values of the time constant (τ) and diffusion length (L) according to Eq. (17). Then, we give an estimation of the Ga diffusion coefficient through the GaN sublayer, according to the relation $L = \sqrt{D\tau}$.^{22,23} The measurements of Ga diffusion coefficient are given in Table 3. We notice an increase of the Ga diffusion length versus growth temperature. This means an increase of the transient regime duration, for which we associate an equivalent thickness given by $E = 2Ln(10)L$ corresponding to a relative growth rate variation of 1%, according to Eq. (17). The equivalent thickness of the layer increases accordingly from 239 to 372 nm in the growth temperature range of 750°C to 900°C. These results explain why the relatively high initial growth rate is the sum of two contributions of the Ga supplied by TMGa and Ga diffused from the GaAs substrate. We also notice that the Ga diffusion coefficient in GaN increases versus the growth temperature. Figure 10 shows the Arrhenius plot of the diffusion coefficient versus the inverse of temperature according to the following law:^{22–24}

Table 3 Time constant, diffusion lengths (and equivalent thickness given by $E = 2Ln(10)L$ corresponding to $v - v_s = 10^{-2}v_s$), and Ga diffusion coefficient (given by $L = \sqrt{D\tau}$) related to layers A-D.

Layer	Temperature (°C)	Time constant τ (s)	Diffusion length L (μm)	Equivalent thickness E (μm)	Ga diffusion coefficient D ($\times 10^{-13}$ cm^2/s)
A	750	54	0.052	0.239	5.007
B	800	64	0.062	0.285	6.006
C	850	85	0.078	0.358	7.177
D	900	88	0.081	0.372	7.455

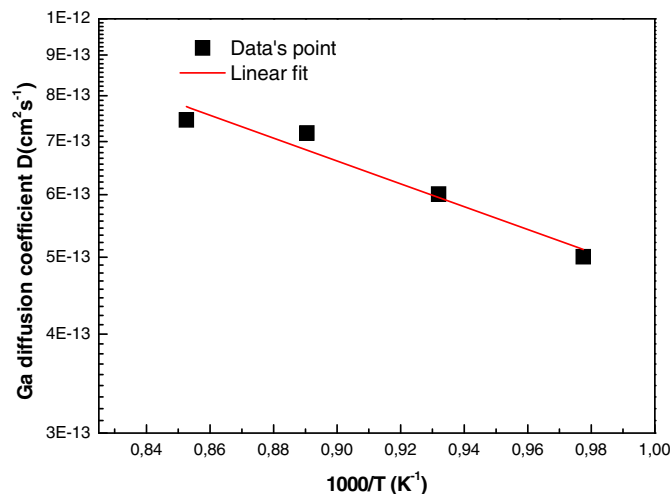


Fig. 10 Arrhenius plot of the Ga diffusion coefficient in the temperature range (750°C to 900°C).

$$D = D_0 \exp\left(-\frac{E_a}{K_B T}\right), \quad (20)$$

where D_0 is a constant, K_B is the Boltzmann constant, and E_a is an activation energy.

The best fit gives the Arrhenius law as follows:

$$D = (1.35 \pm 0.02) 10^{-11} \text{ cm}^2 \text{ s}^{-1} \exp\left(-\frac{(0.28 \pm 0.04) \text{ eV}}{K_B T}\right). \quad (21)$$

This law characterizes the Ga self-diffusion in the GaN layer being deposited on the GaAs (110) substrate. The values of the Ga self-diffusion coefficient in GaN given in this study were in the range of 10^{-13} to 10^{-12} $\text{cm}^2 \text{ s}^{-1}$ at a temperature range of 750-900°C. These values are of the same order of magnitude of 10^{-10} to 10^{-14} $\text{cm}^2 \text{ s}^{-1}$ as the Ga-Al interdiffusion coefficients experimentally found in annealed GaN/AlN at a temperature of about 1000°C to 1100°C.²⁵ Nevertheless, these values are higher than that calculated in a prior reference²⁶ for diffusion of Ga in GaN via a vacancy mediated mechanism, which reported about 10^{-26} to 10^{-17} $\text{cm}^2 \text{ s}^{-1}$ at a temperature range of 850°C to 1300°C. In fact, the theoretical predictions did not take into account the Ga diffusion through dislocations and extended defects emerging from the GaN/GaAs interface. This reason explains the difference between Ga self-diffusion coefficient values given by our approach and those given by a theoretical calculus. This assumption was confirmed by experiments of the nitridation of a 50 nm thick GaN buffer layer for 10 min, which causes the formation of a high density of GaN islands, indicating a local reaction between ammonia and Ga coming from the GaAs substrate. Growth on such a nitrided GaN buffer layer using the same growth conditions of layer C led to the complete disappearance of the growth rate profile. However, this approach deviates from the standard growth process because it led to lower optical qualities. Growth experiments must be performed on GaN/GaAs (110) with lower extended defects to further give experimental identification of Ga self-diffusion mechanisms in GaN.

6 Conclusion

Simulations of the *in situ* reflectance-time curves of GaN/GaAs (110) layers grown by MOVPE at different temperature (750°C to 900°C) were successively performed using an optical model with appropriate interdependent growth rate and surface roughness profiles. The presence of the transient regime in the early stages of GaN growth was associated with Ga diffusion from GaAs (110) due to its thermal decomposition under the used growth conditions. The thermal decomposition of GaAs was enhanced using hydrogen as the carrier gas and a high growth temperature. The quantitative study was conducted given the measurements of a constant time and a diffusion length corresponding to the transient regime during the early stages of MOVPE of GaN on GaAs (110) substrate. These measurements led to an estimation of the Ga self-diffusion coefficient in GaN varying in the range of 10^{-13} to 10^{-12} $\text{cm}^2 \text{ s}^{-1}$ in the temperature range of 750°C to 900°C. As future work, we will consider the self-diffusion mechanisms by an appropriate choice of growth conditions, such as a lower growth temperature (<750°C), which leads to a continuous and 2D GaN layer. By keeping the growth temperature constant and varying the TMGa flux rate and layer thickness, we hope to have a correlation between the mechanisms of diffusion and the dislocation density. This study could be supported by XRD-rocking curves, TEM, and XPS analyses. We will also consider the Ga self-diffusion in GaN for several orientations of GaAs substrates that exhibit different degrees of thermal stability.

Code and Data Availability

Derived data supporting the findings of this study are available from the corresponding author upon request.

Author Contributions

Safa Othmani, Imen Daldoul, Nouredine Chaaben, and Jean Paul Salvestrini wrote the manuscript. The manuscript was written through contributions of all authors. All authors have given approval to the final version of the manuscript.

References

1. S. Ananthanasarn and H. Hasegawa, "Surface passivation of GaAs by ultra-thin cubic GaN layer," *J. Appl. Surf. Sci.* **159–160**, 456–461 (2000).
2. P. Suwanyangyaun, S. Sanorpim, and K. Onabe, "Selective-area growth and characterization of cubic GaN grown by metalorganic vapor phase epitaxy," *Thin Solid Film* **709**, 138125 (2020).
3. J. V. Thordson, O. Zsebök, and T. G. Andersson, "Surface reconstruction and surface morphology of GaN grown by MBE on GaAs (001)," *Phys. Scr.* **79**, 198–201 (1999).
4. Y. Kumagai et al., "*In situ* gravimetric monitoring of halogen transport atomic layer epitaxy of cubic-GaN," *Appl. Surf. Sci.* **159–160**, 427–431 (2000).
5. I. Daldoul et al., "Growth and characterization of cubic GaN grown on GaAs (110) substrate by MOVPE," *Mater. Sci. Semicond. Process.* **132**, 105909 (2021).
6. C. Liu and I. M. Watson, "Quantitative simulation of *in situ* reflectance data from metal organic vapour phase epitaxy of GaN on sapphire," *Semicond. Sci. Technol.* **22**, 629–635 (2007).
7. D. E. Aspnes and A. A. Studna, "Dielectric functions and optical parameters of Si, Ge, GaP, GaAs, GaSb, InP, InAs, and InSb from 1.5 to 6.0 eV," *Phys. Rev B.* **27**(2), 985–1009 (1983).
8. W. G. Breiland and K. P. Killeen, "A virtual interface method for extracting growth rates and high temperature optical constants from thin semiconductor films using *in situ* normal incidence reflectance," *J. Appl. Phys.* **78**, 6726–6736 (1995).
9. R. S. Balmer et al., "Modelling of high temperature optical constants and surface roughness evolution during MOVPE growth of GaN using *in-situ* spectral reflectometry," *J. Cryst. Growth* **245**, 198–206 (2002).
10. J. Szczyrbowski, "Determination of optical constants of real thin films," *J. Phys. D: Appl. Phys.* **11**, 583–593 (1978).
11. N. Chaaben et al., "Simulation of *in situ* reflectance-time during MOVPE of GaN on sapphire substrate," *Superlattices Microstruct.* **64**, 518–534 (2013).
12. J. Laifi et al., "Investigations of *in situ* reflectance of GaN layers grown by MOVPE on GaAs (0 0 1)," *Superlattices Microstruct.* **86**, 472–482 (2015).
13. J. Laifi et al., "Effect of GaAs substrate orientation on the growth kinetic of GaN layer grown by MOVPE," *Superlattices Microstruct.* **94**, 30–38 (2016).
14. H. D. Palfrey, M. Brown, and A. F. W. Willoughby, "Self-diffusion of gallium in gallium arsenide," *J. Electrochem. Soc.* **128**, 2224–2228 (1981).
15. O. Ambacher et al., "Nitrogen effusion and self-diffusion in Ga¹⁴N/Ga¹⁵N isotope heterostructures," *Jpn. J. Appl. Phys.* **37**(5R), 2416–2421 (1998).
16. D. P. Xu et al., "Gallium diffusion through cubic GaN films grown on GaAs(100) at high-temperature using low-pressure MOVPE," *J. Cryst. Growth* **191**(4), 646–650 (1998).
17. K. M. Song et al., "Characteristics of GaN grown by metalorganic chemical vapor deposition using trimethylgallium and triethylgallium," *J. Cryst. Growth* **233** (3), 439–445 (2001).
18. H. X. Wang et al., "Influence of carrier gas on the morphology and structure of GaN layers grown on sapphire substrate by six-wafer metal organic chemical vapor deposition system," *J. Cryst. Growth* **233**(4), 681–686 (2001).
19. N. Itagaki et al., "Growth of single crystalline films on lattice-mismatched substrates through 3D to 2D mode transition," *Sci. Rep.* **10**, 4669 (2020).
20. S. Shokhovets et al., "Reflectivity study of hexagonal GaN films grown on GaAs: surface roughness, interface layer, and refractive index," *J. Appl. Phys.* **84**, 1561–1566 (1998).
21. R. Goldhahn et al., "Determination of group III Nitride film properties by reflectance and spectroscopic ellipsometry studies," *Phys. Status Solidi (a)* **177**(1), 107–115 (2000).
22. M. Pristovsek, F. Poser, and W. Richter, "The impact of the surface on step-bunching and diffusion of Ga on GaAs (001) in metal-organic vapour phase epitaxy," *Mater. Res. Express.* **3**, 075902 (2016).
23. M. Pristovsek et al., "Diffusion of Ga on the GaAs (113) surface in the [110] direction during MOVPE growth," *Appl. Surf. Sci.* **166**, 433–436 (2000).
24. L. Wang et al., "Gallium self-diffusion in gallium phosphide," *Appl. Phys. Lett.* **70**, 1831–1833 (1997).
25. N. Chaaben et al., "Study of Al diffusion in GaN during metal organic vapor phase epitaxy of AlGa_xN/GaN and AlN/GaN structures," *Mater. Sci. Semicond. Process.* **42**, 359–363 (2016).
26. I. A. Aleksandrov et al., "Diffusion in GaN/AlN superlattices: DFT and EXAFS study," *Appl. Surf. Sci.* **515**, 146001 (2020).

Biographies of the authors are not available.